

# A Fixed-Charge Control Strategy of Trans-critical CO<sub>2</sub> Rankine Cycle

Bentao Guo<sup>1,\*</sup>, Vincent Lemort<sup>1</sup>, Aitor Cendoya<sup>1</sup>

<sup>1</sup> *Thermodynamics Laboratory, Aerospace and Mechanical Engineering Department, Faculty of Applied Sciences, University of Liège, Belgium*

\*Corresponding Author: [Bentao.Guo@uliege.be](mailto:Bentao.Guo@uliege.be)

## ABSTRACT

The trans-critical CO<sub>2</sub> Rankine cycle (TCRC) is an effective solution for waste heat recovery and Carnot battery applications, especially when combined with sensible heat storage and operating over a wide temperature range. However, controlling the cycle can be complex, as its performance depends heavily on selecting an appropriate high pressure. This study proposes a fixed-charge control strategy for TCRC. Instead of adjusting the high pressure in real-time, the optimal refrigerant charge is selected and maintained constant throughout operation, which is determined under an intermediate condition defined by the cooling water and thermal oil supply temperatures. The relationship between high pressure, running charge, and thermal efficiency is illustrated, and the optimum charge distribution under various conditions is presented. Then, the fixed-charge strategy is compared to the conventional optimum-high-pressure approach in a TCRC equipped with a liquid reservoir. Around the intermediate condition, both methods yield similar thermal efficiency. A refrigerant reservoir can be added between the gas heater and the expander to improve performance over a wider range of conditions. This modification reduces the maximum absolute deviation in thermal efficiency to only 0.19 %. This work supplies a simpler alternative control strategy for TCRCs, reducing system complexity while maintaining high performance.

## 1 INTRODUCTION

Energy storage technologies are becoming more and more crucial (Wang *et al.*, 2022b), compensating for the intermittent nature of variable renewable energy, and among them, pumped thermal energy storage (Carnot battery), where electric energy is stored as thermal energy and later recovered during discharge (Guo *et al.*, 2025), outstands due to its flexible capacity, long lifetime and minimal dependency on geological sites or resources. Large-scale trans-critical CO<sub>2</sub> Carnot batteries have been investigated with Technology Readiness Level up to 3–4 (Shamsi *et al.*, 2024) and demonstrate better technical and economic performance than other energy storage technologies with sensible hot storage, with a highest predicted round-trip-efficiency up to 68 % and a lowest capital cost (Zhao *et al.*, 2022). The trans-critical CO<sub>2</sub> heat pump systems have been investigated and applied in many applications, for instance, residential water heaters (Wang *et al.*, 2022a), refrigeration (Sacacas *et al.*, 2022) and automotive thermal management systems (Jia *et al.*, 2024), and trans-critical CO<sub>2</sub> Rankine cycles (TCRC) get less attention compared to the heat pumps, although they perform better than organic Rankine cycle at high heat source temperature (Astolfi *et al.*, 2018; Wieland *et al.*, 2023). TCRCs are important when coupled with a CO<sub>2</sub> heat pump in a reversible Carnot battery with low-temperature cold storage, which needs to be investigated further (Shamsi *et al.*, 2024) or in other situations, such as solar-thermal power plants (Chen *et al.*, 2010).

It has been proved that high pressure is key to the TCRC performance (efficiency and output), and there is an optimum high pressure for the largest net power output (Ahmadi *et al.*, 2017; Li *et al.*, 2018a; Song *et al.*, 2020; Zhao *et al.*, 2020) or system efficiency (Cayer *et al.*, 2009; Chen and Lundqvist, 2011; Li *et al.*, 2014), as presented in Table 1, where the high pressure range varies with operational conditions. In the operational control of the current TCRC, the working fluid mass flow rate is

controlled by adjusting the working fluid pump speed, and the optimum operation pressure is achieved by adjusting the expansion equipment capacity or working fluid pump speed, leading to the low robustness of the system. In the experimental work of Li *et al.* (2018b), the opening of the expansion valve (replacing the speed of an expander) is adjusted to change the high pressure. In practice, the high pressure in a designed TCRC can be controlled according to the performance map or correlation to the condition parameters, although there are not many available correlations yet. In the dynamic simulation of Wang *et al.* (2020), the high pressure is adjusted by the optimal pump speed, which is gained from operational map for the maximum net power output. The optimum high pressure is also mapped under various conditions, and it is achieved by the adjustable stator angle of the turbine in Du *et al.* (2018). In the experiment of Li *et al.* (2017), the high pressure is changed by the control function with the heat source flow rate and CO<sub>2</sub> mass flow rate. For the trans-critical CO<sub>2</sub> heat pump system, some researchers propose new control strategies by charge management, so that the expansion valve does not control the high pressure but only controls the overheating degree (He *et al.*, 2020). In the TCRC, the charge distribution regulation can also be concluded, and then a similar control strategy can be utilized to simplify or neglect the control of the optimum high pressure.

**Table 1:** Summary of the TCRC optimum range of high pressure

Ref.	Recuperative?	Control goal	High pressure
Ahmadi <i>et al.</i> (2017)	No	Net power/Efficiency	9-10 MPa
Li <i>et al.</i> (2018a)	Yes	Net power	13-14 MPa
Song <i>et al.</i> (2020)	Yes	Net power	13-15 MPa
Zhao <i>et al.</i> (2020)	Yes	Net power/Efficiency	15 MPa
Cayer <i>et al.</i> (2009)	Yes/No	Efficiency	11 MPa/14 MPa
Chen and Lundqvist (2011)	No	Efficiency	11-18 MPa
Li <i>et al.</i> (2014)	Yes/No	Efficiency	10-12 MPa/11-15 MPa

In this study, the charge distribution variation in a TCRC with the secondary fluid (thermal oil and cooling water) temperature is presented, and a fixed-charge control strategy is proposed to compare with the optimal system with the optimum high pressure. In Section 2, the detail of the studied system is given, and the models and control strategies are presented. In Section 3, the relationship between the TCRC performance, its optimum expander inlet pressure, and system charge is illustrated, and the performance of the fixed-charge control strategy is analyzed and improved by comparing it with optimum-high-pressure operation.

## 2 METHODOLOGY

### 2.1 Studied TCRC system

The studied basic TCRC is a part of a reversible CO<sub>2</sub> heat pump/power cycle coupled with a reverse-osmosis system in Ben Guerir, Morocco, which is a case study in the ‘REPTES’ project, and its power cycle is shown in Figure 1. During the day, the heat pump heats the thermal oil and cools down the well water, storing it in a hot storage tank and a water tank, respectively. The oil and cold water stored are used as secondary fluids for the TCRC at night when irrigation pumps operate. Due to the irrigation requirements, the cooling water flow rate is fixed as 3 m<sup>3</sup> / h, and its supply temperature fluctuates with the heat pump operation. An identical commercial scroll compressor (Li *et al.*, 2023) in the CO<sub>2</sub> automotive heat pump (Volkswagen, 2021) is used as the expander. The designed sizes are presented in Table 2, which are used as parameters for the off-design model.

### 2.2 Charge-sensitive model

A charge-sensitive off-design model (Dickes *et al.*, 2018) for a trans-critical TCRC (Dumont *et al.*, 2018) is built in MATLAB environments, and the fluid properties are calculated by CoolProp (Bell *et al.*, 2014). The performance of expanders is calculated by a semi-empirical expander model (Lemort *et al.*, 2009). The heat exchange process is divided into 150 microelements in the gas heater, considering the dramatic density change in the supercritical state. The correlations of heat transfer and friction

pressure drop in heat exchangers are listed in Table 3. Note that a homogeneous void fraction model (Wu and Duan, 2019) is used because the density difference of saturated vapor and liquid is smaller compared to other refrigerants (He *et al.*, 2020).

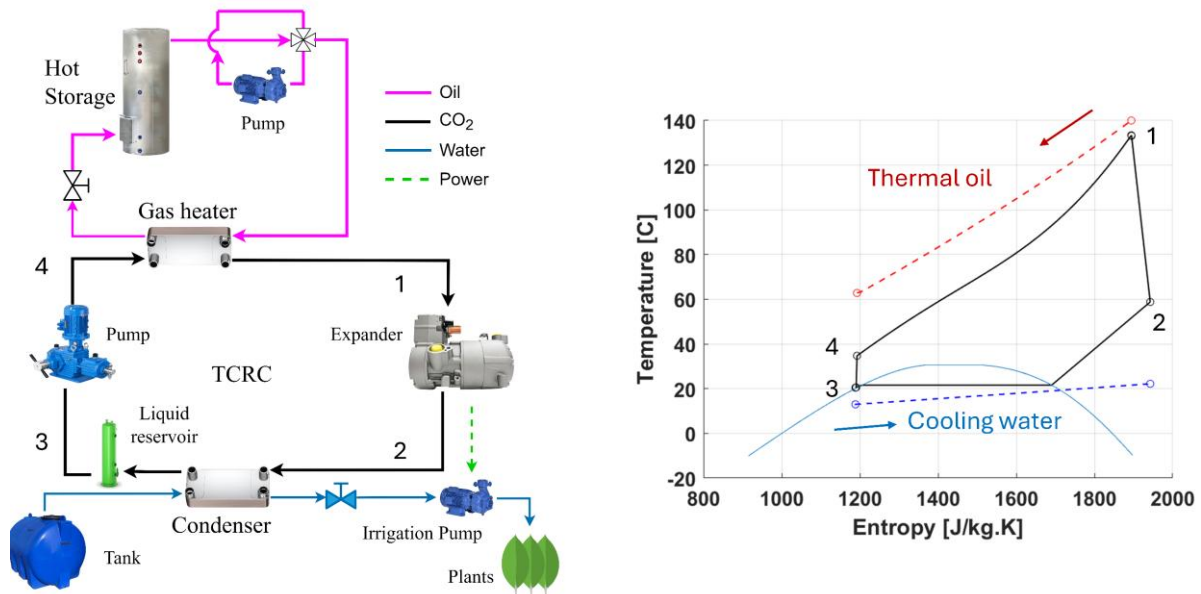


Figure 1: TCRC system layout and T-S diagram

Table 2: Size parameters of the studied TCRC

Expander		Heat exchangers	
Type	Scroll	Type	Brazed plate heat exchanger
Swept volume	5.36 cm <sup>3</sup>	Gas heater:	
Built-in volume ratio	2.26	Plate numbers	23
Speed range	600-8600 rpm	Length/width	0.519 m / 0.252 m
<b>CO<sub>2</sub> pump</b>		Internal volume	1.679 L
Type	Plunger	Condenser:	
Swept volume	14.5 cm <sup>3</sup>	Plate numbers	26
Isentropic efficiency	0.95	Length/width	0.42 m / 0.165 m
Volumetric efficiency	0.95	Internal volume	1.243 L
Nominal speed	1450 rpm		

Table 3: Correlations in the off-design model

Gas heater		Pressure drops
Supercritical CO <sub>2</sub>	Forooghi and Hooman (2014)	Lee <i>et al.</i> (2020)
Thermal oil	Lee <i>et al.</i> (2020)	/
Condenser		
Vapor/Liquid CO <sub>2</sub>	Martin (1996)	Martin (1996)
Two-phase CO <sub>2</sub>	Kondou and Hrnjak (2011)	Tao and Ferreira (2019)
Water	Martin (1996)	/

The running charge amount is calculated by:

$$M_{run} = M_{GH} + M_{CD} + M_{exp} + M_{pp} \quad (1)$$

The total charge amount is calculated by (the charge in pipes is assumed as 0):

$$M_{tot} = M_{run} + M_{LR} + M_{RR} \quad (2)$$

In the gas heater, the mass of the super-critical CO<sub>2</sub> is calculated by:

$$M_{GH} = \int_0^{V_{GH}} \rho dV \quad (3)$$

The refrigerant mass of other components is from Dickes *et al.* (2018). Models of a liquid reservoir (LR) and a vapor-refrigerant reservoir (RR) are built (Dickes *et al.*, 2018) as their function is discussed in this study. The optimum high pressure and optimum running charge in this work refer to the values at the highest thermal efficiency, rather than net power output, because the studied TCRC is coupled into a Carnot battery, and its thermal efficiency is related to the consumption of hot storage and the requirement for heat pump performance. The thermal efficiency of the TCRC is:

$$\eta_{th} = (\dot{W}_{exp} - \dot{W}_{pp}) / \dot{Q}_{gh} \quad (4)$$

The optimum-high-pressure system is to regulate the system operating at its optimum high pressure (the searching step is 5 bar). The fixed-charge control strategy is that the charge of the system is set as the optimum charge at the intermediate values ( $T_h=120$  °C,  $T_w=17$  °C) of various thermal oil (110 – 130 °C) and cooling water (13 – 21 °C) temperatures, and the refrigerant status will get a balance by itself. The CO<sub>2</sub> pump speed is set to be 800 rpm. The subcooling degree at the condenser outlet is fixed at a low value, 1 K, to investigate the performance of the fixed charge.

### 3 RESULTS AND DISCUSSIONS

#### 3.1 Relationship of high pressure and charge in TCRC

Under three operation conditions ( $T_h = 120$  °C,  $T_w = 13$  °C;  $T_h = 120$  °C,  $T_w = 17$  °C;  $T_h = 130$  °C,  $T_w = 17$  °C), the variation of the TCRC performance with the expander inlet pressure and the corresponding running charge is presented in Figure 2. The charge amount is nearly proportional to the high pressure, and the optimum high pressure exists but differs under various conditions. The optimum running charge amount and the optimum high pressure appear simultaneously, meaning that the optimum running charge is the working fluid mass corresponding to the high pressure of maximum system efficiency. Note that the optimum high pressure also varies with the efficiencies of the expander and CO<sub>2</sub> pump.

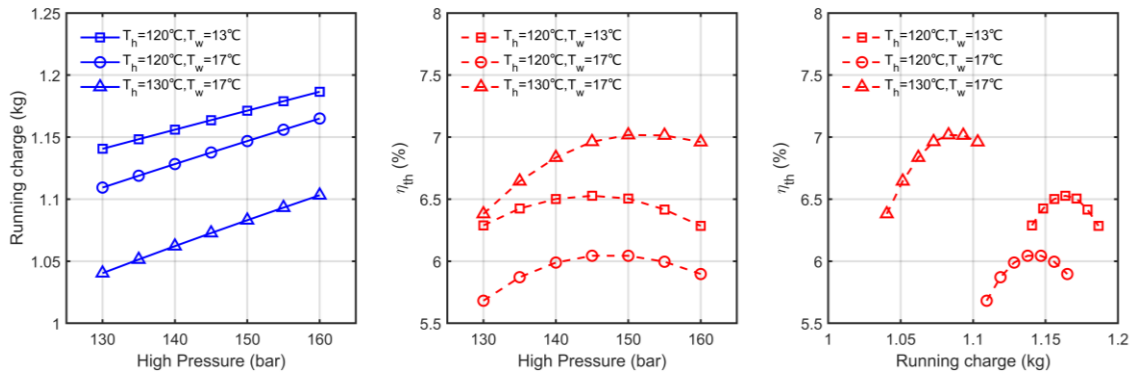


**Figure 2:** Relationship of high pressure, thermal efficiency, and running charge

The optimum running charge distribution in TCRC is presented in Figure 3. The charge in the expander and pump can be negligible compared to that in the condenser and gas heater. The optimum running charge under the intermediate condition is 1.138 kg, as highlighted in Figure 3. When  $T_h = 120$  °C, the charge in the condenser and gas heater increases and decreases with the rising  $T_w$ , respectively, and the reduction in the gas heater is larger as the total running charge also drops. When  $T_w = 17$  °C, the charge amounts in the condenser and gas heater both decrease with the rising  $T_h$ , and the decline in the gas heater is larger. The charge reduction in the condenser is little, from 0.435 kg to 0.426 kg, with the  $T_h$  rising from 110 °C to 130 °C. In summary, the charge of the gas heater is more sensitive to the water and thermal oil supply temperature, unlike the CO<sub>2</sub> heat pump water heater (He *et al.*, 2020).

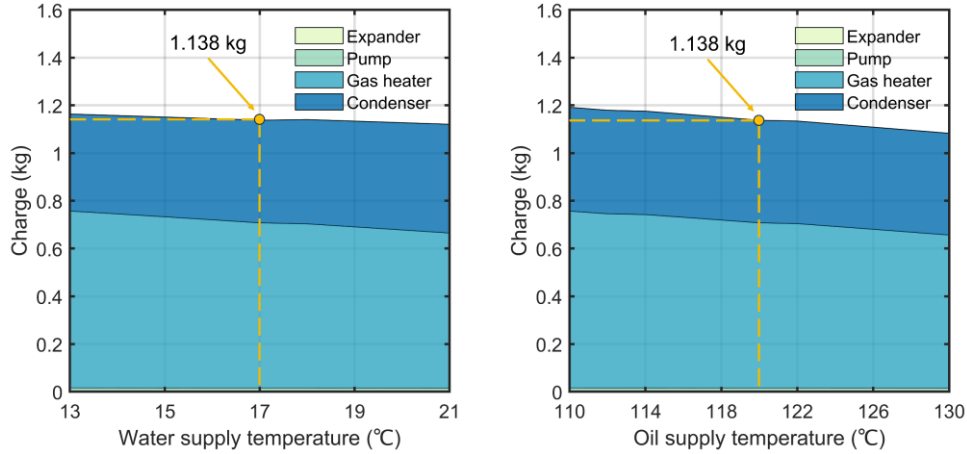


**Figure 3:** Optimum charge distribution on various conditions (left:  $T_h=120^\circ\text{C}$ , right:  $T_w=17^\circ\text{C}$ )

### 3.2 Comparison of the control strategies

Usually, in the organic Rankine cycles (Desideri *et al.*, 2017; Ziviani *et al.*, 2018) and TCRCs (Li *et al.*, 2022; Wang *et al.*, 2020), there is a liquid reservoir between the condenser and the pump, so the performance of the fixed-charge control strategy in a TCRC with an LR ( $V_{LR} = 0.8$  L) is analyzed in this section. Figure 4 shows the comparison of the thermal efficiency in fixed-charged and optimum-pressure TCRC under various  $T_w$  and  $T_h$ .

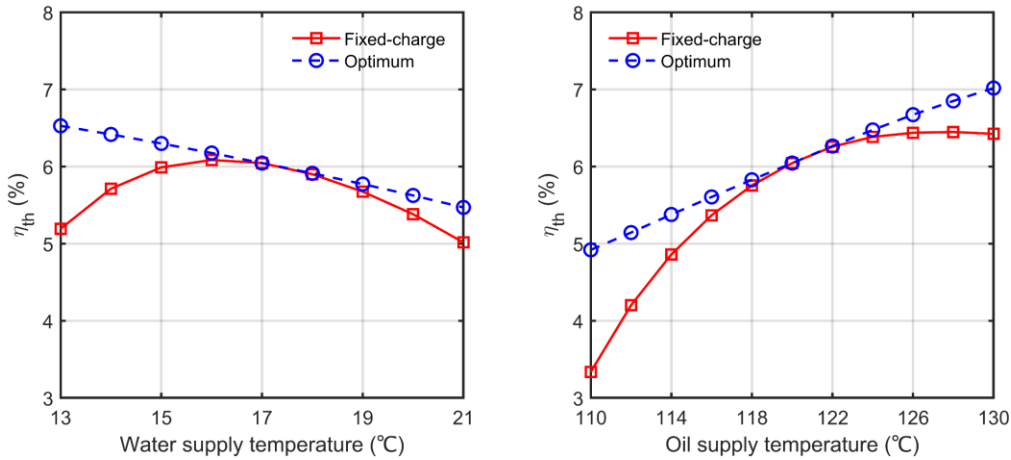


**Figure 4:** Thermal efficiency comparison with a liquid reservoir (0.8 L)

Near the intermediate point ( $T_h = 118 - 125^\circ\text{C}$ ,  $T_w = 16 - 19^\circ\text{C}$ ), the fixed-charge control gets almost the same performance as the optimum-pressure one, but when the operation condition is far away from the selected point, the absolute deviation of  $\eta_{th}$  becomes larger, up to 1.3 % when  $T_h = 120^\circ\text{C}$  and  $T_w = 13^\circ\text{C}$ , and 1.56 % when  $T_h = 110^\circ\text{C}$  and  $T_w = 17^\circ\text{C}$ . A larger variation occurs at the extremes of the operating window because the operational pressure of the gas heater changes more. For instance, the optimum high pressure when  $T_h = 110^\circ\text{C}$  and  $T_w = 17^\circ\text{C}$  is 140 bar, and the high pressure in the fixed-charge operation is 110 bar. When  $T_h = 120^\circ\text{C}$  and  $T_w = 13^\circ\text{C}$ , the operational high pressures are 145 bar and 113 bar, respectively, in the optimum-pressure and fixed-charged control.

### 3.3 Improvement of the fixed-charge control

A vapor-refrigerant (note that the phase of the inside refrigerant is supercritical) reservoir of  $V_{RR} = 1$  L is introduced to balance the charge amount of the condenser, which varies significantly with the  $T_w$ . It can be put after GH (between the gas heater and the expander) or before GH (between the pump and

the gas heater) (He *et al.*, 2020). The liquid reservoir is kept, but its volume is reduced to 0.2 L. Figure 5 shows the comparison of the thermal efficiency in fixed-charge and optimum-pressure TCRC under various  $T_h$  and  $T_w$ . Compared to Figure 4, where there is only LR, the fixed-charge TCRC with a refrigerant reservoir performs better and closer to the optimum-pressure one, and the solution with the RR after GH performs better than that with RR before GH because its high pressure is closer to the optimum value. The maximum absolute deviation of  $\eta_{th}$  with a fixed-charge control and RR after GH is only 0.44 %, and this value can be 0.19 % when  $V_{RR}$  is enlarged to 5 L, but the total charge amount increases from 1.576 kg to 2.734 kg.

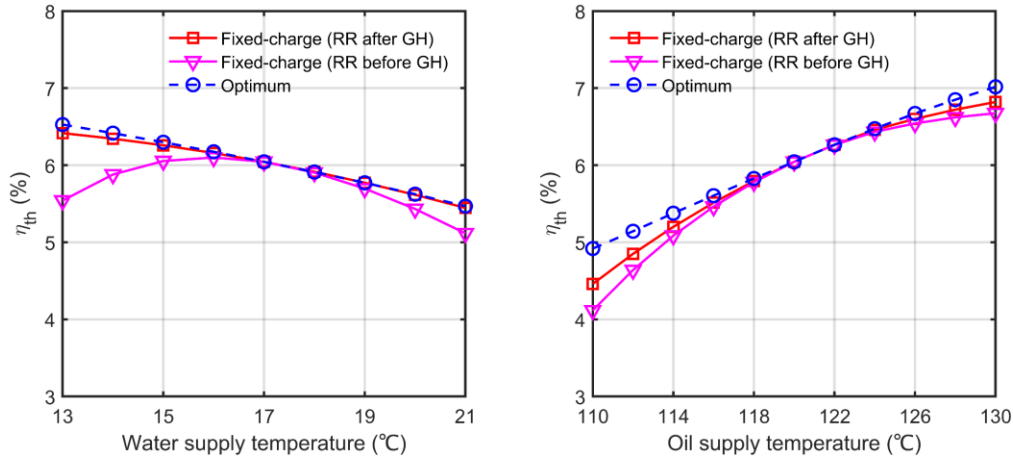


**Figure 5:** Thermal efficiency comparison with a refrigerant reservoir (1 L) + LR (0.2 L)

Four operation conditions are selected to verify the performance when neither  $T_h$  nor  $T_w$  is located at the intermediate point, as shown in Table 4. The optimum-pressure system works at the optimum high pressure and total charge amount, as listed in Table 4, and the fixed-charge system works at a total charge of 1.576 kg.

**Table 4:** Four conditions deviated from the intermediate condition

No.	1	2	3	4
$T_h$ / °C	115	125	115	125
$T_w$ / °C	15	15	19	19
Optimum high pressure / bar	150	145	150	150
Optimum total charge / kg	1.667	1.603	1.570	1.530

The performance under these four conditions of the fixed-charge TCRC with or without RR is illustrated in Figure 6, and the fixed-charge TCRC with RR after GH performs better. The maximum absolute deviation of the  $\eta_{th}$  is decreased from 1.40 % to 0.19 %. Moreover, the maximum relative deviation of the net power output is reduced from 16 % to 5 % (occurring under the fourth condition in Table 4) when a “RR after GH” solution replaces the “only LR” solution. Note that the net power out of the fixed-charge operation of both above solutions under the second and third conditions is almost the same as the optimum-pressure operation.

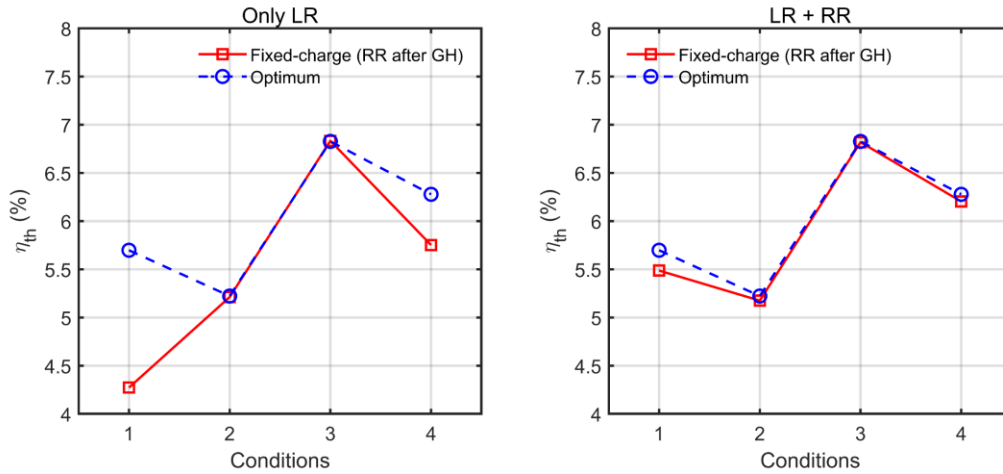


**Figure 6:** Performance of “only LR” and “RR after GH” under the conditions in Table 4

## 4 CONCLUSIONS

A fixed-charge control strategy is proposed based on the optimum charge under the intermediate operation condition in a trans-critical CO<sub>2</sub> Rankine cycle (TCRC), and its performance is verified by comparing it with the conventional optimum-pressure control. The main conclusions are as follows:

- The running charge amount increases monotonically with the high pressure (expander inlet pressure) in the TCRC, and the optimum running charge and optimum high pressure appear simultaneously. The charge amount in the gas heater is sensitive to the heat source temperature and the heat sink temperature.
- In the TCRC with a liquid reservoir, the fixed-charge control strategy performs similarly only near the intermediate condition, and the absolute deviation of  $\eta_{th}$  is up to 1.56 % at  $T_h = 110$  °C and  $T_w = 17$  °C.
- By introducing a refrigerant reservoir between the gas heater and the expander, the fixed-charge performance can be improved, and the maximum absolute deviation of the  $\eta_{th}$  is only 0.19 % when both  $T_h$  and  $T_w$  deviate from the intermediate condition.

The brief comparison of the proposed fixed-charge control strategy and the previous optimum-pressure operation is concluded in Table 5.

**Table 5:** Comparison of the fixed-charge and optimum-pressure operation

	Fixed charge	Optimum pressure
Implementation	To decide the optimum charge of the intermediate operational point in the design process	To adjust the high pressure in the off-design stage according to the control correlations or maps
Off-design operation	None	To adjust the pump speed or expander capacity
Control goal	Mass flow rate	Mass flow rate, high pressure
Performance	No evident performance drop compared to the optimal point	Optimal performance
Advantage	Simpler operation	Better performance
Drawback	A little performance decrement	More complex operation

This control strategy can simplify the control of the trans-critical CO<sub>2</sub> Rankine cycle, eliminating the control for the optimum high pressure, if the system charge amount is set to be the optimum charge at the intermediate point of the possible operation conditions. In future work, the volume of the refrigerant reservoir and liquid reservoir can be optimized.



## NOMENCLATURE

M	charge amount	(kg)
$\dot{Q}$	heat transfer	(W)
T	temperature	(°C)
V	volume	(liter)
$\dot{W}$	power	(W)
$\eta$	efficiency	(–)

### Subscript

CD	condenser
exp	expander
GH	gas heater
h	hot thermal oil
LR	liquid reservoir
pp	working fluid pump
RR	refrigerant reservoir
w	water

## REFERENCES

- Ahmadi, M. H., Mehrpooya, M., Abbasi, S., Pourfayaz, F., Bruno, J. C., 2017, Thermo-economic analysis and multi-objective optimization of a transcritical CO<sub>2</sub> power cycle driven by solar energy and LNG cold recovery, *Thermal Science and Engineering Progress*, vol. 4, p. 185-196.
- Astolfi, M., Alfani, D., Lasala, S., Macchi, E., 2018, Comparison between ORC and CO<sub>2</sub> power systems for the exploitation of low-medium temperature heat sources, *Energy*, vol. 161, p. 1250-1261.
- Bell, I. H., Wronski, J., Quoilin, S., Lemort, V., 2014, Pure and pseudo-pure fluid thermophysical property evaluation and the open-source thermophysical property library CoolProp, *Industrial & engineering chemistry research*, vol. 53, 6: p. 2498-2508.
- Cayer, E., Galanis, N., Desilets, M., Nesreddine, H., Roy, P., 2009, Analysis of a carbon dioxide transcritical power cycle using a low temperature source, *Applied Energy*, vol. 86, 7-8: p. 1055-1063.
- Chen, Y., Pridasawas, W., Lundqvist, P., 2010, Dynamic simulation of a solar-driven carbon dioxide transcritical power system for small scale combined heat and power production, *Solar Energy*, vol. 84, 7: p. 1103-1110.
- Chen, Y., Lundqvist, P., The CO<sub>2</sub> transcritical power cycle for low grade heat recovery: Discussion on temperature profiles in system heat exchangers, *ASME Power Conference*, p. 385-392
- Desideri, A., Zhang, J., Kærn, M. R., Ommen, T. S., Wronski, J., Lemort, V., Haglind, F., 2017, An experimental analysis of flow boiling and pressure drop in a brazed plate heat exchanger for organic Rankine cycle power systems, *International Journal of Heat and Mass Transfer*, vol. 113, p. 6-21.
- Dickes, R., Dumont, O., Guillaume, L., Quoilin, S., Lemort, V., 2018, Charge-sensitive modelling of organic Rankine cycle power systems for off-design performance simulation, *Applied energy*, vol. 212, p. 1262-1281.
- Du, Y., Chen, H., Hao, M., Qiang, X., Wang, J., Dai, Y., 2018, Off-design performance comparative analysis of a transcritical CO<sub>2</sub> power cycle using a radial turbine by different operation methods, *Energy Conversion and Management*, vol. 168, p. 529-544.
- Dumont, O., Dickes, R., De Rosa, M., Douglas, R., Lemort, V., 2018, Technical and economic optimization of subcritical, wet expansion and transcritical Organic Rankine Cycle (ORC) systems coupled with a biogas power plant, *Energy Conversion and Management*, vol. 157, p. 294-306.
- Forooghi, P., Hooman, K., 2014, Experimental analysis of heat transfer of supercritical fluids in plate heat exchangers, *International Journal of Heat and Mass Transfer*, vol. 74, p. 448-459.
- Guo, B., Lemort, V., Cendoya, A., 2025, Control strategy and techno-economic optimization of a small-scale hybrid energy storage system: A reversible HP/ORC-based Carnot battery and an electrical battery, *Energy*, vol. 329, p. 136508.



- He, Y.-J., Liang, X.-Y., Cheng, J.-H., Shao, L.-L., Zhang, C.-L., 2020, Approaching optimum COP by refrigerant charge management in transcritical CO<sub>2</sub> heat pump water heater, *International Journal of Refrigeration*, vol. 118, p. 161-172.
- Jia, F., Yin, X., Cao, F., Fang, J., Wang, A., Wang, X., Yang, L., 2024, A novel control method for the automotive CO<sub>2</sub> heat pumps under inappropriate refrigerant charge conditions, *Energy*, vol. 286, p. 129533.
- Kondou, C., Hrnjak, P., 2011, Heat rejection from R744 flow under uniform temperature cooling in a horizontal smooth tube around the critical point, *International Journal of Refrigeration*, vol. 34, 3: p. 719-731.
- Lee, C., Ko, J.-W., Ji, H. Y., Kim, S.-C., 2020, Experimental assessment of convective heat transfer and pressure drop correlation of R1234ze (E) for a supercritical heat exchanger in the organic Rankine cycle, *Journal of Mechanical Science and Technology*, vol. 34, p. 4809-4818.
- Lemort, V., Quoilin, S., Cuevas, C., Lebrun, J., 2009, Testing and modeling a scroll expander integrated into an Organic Rankine Cycle, *Applied Thermal Engineering*, vol. 29, 14-15: p. 3094-3102.
- Li, G., Ma, J., Zou, H., Zhang, R., 2023, Experimental investigation of refrigerant charge determination for heating performance in a CO<sub>2</sub> heat pump system for electric vehicles, *Applied Thermal Engineering*, vol. 233, p. 121147.
- Li, H., Yang, Y., Cheng, Z., Sang, Y., Dai, Y., 2018a, Study on off-design performance of transcritical CO<sub>2</sub> power cycle for the utilization of geothermal energy, *Geothermics*, vol. 71, p. 369-379.
- Li, L., Ge, Y., Luo, X., Tassou, S. A., 2017, Experimental investigation on power generation with low grade waste heat and CO<sub>2</sub> transcritical power cycle, *Energy Procedia*, vol. 123, p. 297-304.
- Li, L., Tian, H., Shi, L., Zhang, Y., Huang, G., Zhang, H., Wang, X., Shu, G., 2022, Experimental investigation of a splitting CO<sub>2</sub> transcritical power cycle in engine waste heat recovery, *Energy*, vol. 244, p. 123126.
- Li, M., Wang, J., Li, S., Wang, X., He, W., Dai, Y., 2014, Thermo-economic analysis and comparison of a CO<sub>2</sub> transcritical power cycle and an organic Rankine cycle, *Geothermics*, vol. 50, p. 101-111.
- Li, X., Shu, G., Tian, H., Huang, G., Liu, P., Wang, X., Shi, L., 2018b, Experimental comparison of dynamic responses of CO<sub>2</sub> transcritical power cycle systems used for engine waste heat recovery, *Energy Conversion and Management*, vol. 161, p. 254-265.
- Martin, H., 1996, A theoretical approach to predict the performance of chevron-type plate heat exchangers, *Chemical Engineering and Processing: Process Intensification*, vol. 35, 4: p. 301-310.
- Sacasas, D., Vega, J., Cuevas, C., 2022, An annual energetic evaluation of booster and parallel refrigeration systems with R744 in food retail supermarkets. A Chilean perspective, *International Journal of Refrigeration*, vol. 133, p. 326-336.
- Shamsi, S. S. M., Barberis, S., Maccarini, S., Traverso, A., 2024, Large scale energy storage systems based on carbon dioxide thermal cycles: A critical review, *Renewable and Sustainable Energy Reviews*, vol. 192, p. 114245.
- Song, J., Li, X., Ren, X., Tian, H., Shu, G., Gu, C., Markides, C. N., 2020, Thermodynamic and economic investigations of transcritical CO<sub>2</sub>-cycle systems with integrated radial-inflow turbine performance predictions, *Applied Thermal Engineering*, vol. 165, p. 114604.
- Tao, X., Ferreira, C. A. I., 2019, Heat transfer and frictional pressure drop during condensation in plate heat exchangers: Assessment of correlations and a new method, *International Journal of Heat and Mass Transfer*, vol. 135, p. 996-1012.
- Volkswagen, 2021, SSP 881213 - Air Conditioning and Heat Pump in MEB Vehicles, 2025, March 5: <https://vw-us.erwin-store.com/erwin/showArticleProperties.do?articleId=185907>
- Wang, J., Belusko, M., Evans, M., Liu, M., Zhao, C., Bruno, F., 2022a, A comprehensive review and analysis on CO<sub>2</sub> heat pump water heaters, *Energy Conversion and Management: X*, vol. 15, p. 100277.
- Wang, R., Shu, G., Wang, X., Tian, H., Li, X., Wang, M., Cai, J., 2020, Dynamic performance and control strategy of CO<sub>2</sub>-mixture transcritical power cycle for heavy-duty diesel engine waste-heat recovery, *Energy Conversion and Management*, vol. 205, p. 112389.
- Wang, W., Yuan, B., Sun, Q., Wennersten, R., 2022b, Application of energy storage in integrated energy systems—A solution to fluctuation and uncertainty of renewable energy, *Journal of Energy Storage*, vol. 52, p. 104812.

- Wieland, C., Schiffelechner, C., Braimakis, K., Kaufmann, F., Dawo, F., Karellas, S., Besagni, G., Markides, C. N., 2023, Innovations for organic Rankine cycle power systems: Current trends and future perspectives, *Applied Thermal Engineering*, vol. 225, p. 120201.
- Wu, H., Duan, Q., 2019, Gas void fraction measurement of gas-liquid two-phase CO<sub>2</sub> flow using laser attenuation technique, *Sensors*, vol. 19, 14: p. 3178.
- Zhao, D., Zhao, R., Deng, S., Zhao, L., Chen, M., 2020, Transcritical carbon dioxide power cycle for waste heat recovery: A roadmap analysis from ideal cycle to real cycle with case implementation, *Energy Conversion and Management*, vol. 226, p. 113578.
- Zhao, Y., Song, J., Liu, M., Zhao, Y., Olympios, A. V., Sapin, P., Yan, J., Markides, C. N., 2022, Thermo-economic assessments of pumped-thermal electricity storage systems employing sensible heat storage materials, *Renewable Energy*, vol. 186, p. 431-456.
- Ziviani, D., James, N. A., Accorsi, F. A., Braun, J. E., Groll, E. A., 2018, Experimental and numerical analyses of a 5 kWe oil-free open-drive scroll expander for small-scale organic Rankine cycle (ORC) applications, *Applied energy*, vol. 230, p. 1140-1156.

### **ACKNOWLEDGEMENTS**

The authors would like to acknowledge the support of the project "REPTES - Renewable plants integrated with pumped thermal energy storage for sustainable satisfaction of energy and agricultural needs of African communities" under LEAP-RE programme, which has received funding from the European Union's Horizon 2020 Research and Innovation Program under Grant Agreement 963530. This work was also supported by the Fonds de la Recherche Scientifique - FNRS under Grant(s) n° R.8003.23.